# A HYBRID OBSERVER FOR THE DRIVELINE DYNAMICS

**Andrea Balluchi[†], Luca Benvenuti[‡], Maria D. Di Benedetto[§], Alberto L. Sangiovanni Vincentelli[†¶]**

[†] PARADES, Via di S.Pantaleo, 66, 00186 Roma, I.
e-mail: balluchi@parades.rm.cnr.it
http://www.parades.rm.cnr.it

[‡]Dip. di Informatica e Sistemistica, Università di Roma "La Sapienza", Via Eudossiana, 18, 00184 Roma, I
e-mail: benvenuti@dis.uniroma1.it
http://www.dis.uniroma1.it

[§]Dip. di Ingegneria Elettrica, Università di L'Aquila, Poggio di Roio, 67040 L'Aquila, I
e-mail: dibenede@ing.univaq.it
http://www.ing.univaq.it

[¶]Dep. of Electrical Engineering and Computer Science, University of California at Berkeley, CA 94720, USA
e-mail: alberto@eecs.berkeley.edu
http://www.eecs.berkeley.edu

**Keywords:** Powertrain control, hybrid systems observers, hybrid systems.

## Abstract

In this paper a methodology for the design of a hybrid observer for a hybrid system with no continuous state reset is proposed. This methodology is applied to the synthesis of a hybrid observer for a model of a driveline with discontinuity in the elastic torsionial coefficient.

## 1 Introduction

Hybrid systems have been the subject of intensive study in the past few years by both the control and the computer science communities. Recently, hybrid system techniques have been applied to an important industrial domain: automotive engine and power–train control (e.g. [1]).

In this domain, the ever increasing computational power of micro controllers has made it possible to extend the functionality of electronic subsystems controlling the motion and the performance of the car to limits that were unthinkable only a few years ago. This opportunity has exposed the need for control algorithms that meet the more and more tighting demands on passengers' comfort, safety, emissions and fuel consumption imposed by car manufacturers and regulations. To cope with this challenge, cycle-accurate models of the engine and the power train, are needed. These models are intrinsically hybrid because, while torque generation and fuel injection are both synchronized with the phases of the pistons and, hence, should be modeled as event-driven systems, power–train and air dynamics can be modeled as continuous-time systems.

In this work we consider control problems related to driveability requirements. Driveability requirements play an important role. In particular, longitudinal car oscillations represent one of the most critical aspects especially when fast torque changes are requested by the driver (tip-in and tip-out). To tackle this problem, active damping of power-train oscillations has been recently proposed (see i.e. [9, 10]). Damping of the oscillations can be achieved by modulation of the generated torque via drive-by-wire actuators, fuel injection and spark ignition control.

By using hybrid system techniques for modeling and synthesis, we recently proposed solutions to several challenging control problems related to driveability such as: the Fast Force Transient problem [3] and the Cut-Off problem [2]. The Cut-Off problem corresponds to the complete release of the gas pedal by the driver. For cars equipped with drive-by-wire electronics, such control problem can be formulated as Fast Force Transient problem. However, for traditional cars, where the throttle valve is directly connected to the gas pedal and there is no possibility of acting on the mass of air loaded by the cylinders, a different approach has to be used. The reduced control authority does not allow us to avoid vehicle oscillations. Indeed, in this case, the goal is to cut–off fuel injection minimizing passengers' discomfort due to the unavoidable power–train oscillations. Both problems have been solved by designing hybrid controllers with power–train full state feedback. Since state measurements are not available, these control laws call for the synthesis of a power–train state observer.

In Section 2, a hybrid model of the driveline that describes the nonlinearities due to discontinuous elasticity is proposed. A hybrid observer for the driveline hybrid model is developed in Section 3 and simulation results are presented.

## 2 Driveline hybrid model

In this work, we consider the dynamics of an automotive power–train with clutch closed and fixed gear. In particular, we concentrate our attention to the case of a low gear selection and small vehicle velocities, where the undesired oscillating behavior of the driveline is more apparent. We studied a very complex 7–dimensional nonlinear model of the power–train developed at Magneti Marelli, Divisione Sistemi Motopropulsione, Italy. Such continuous–time model describes with high

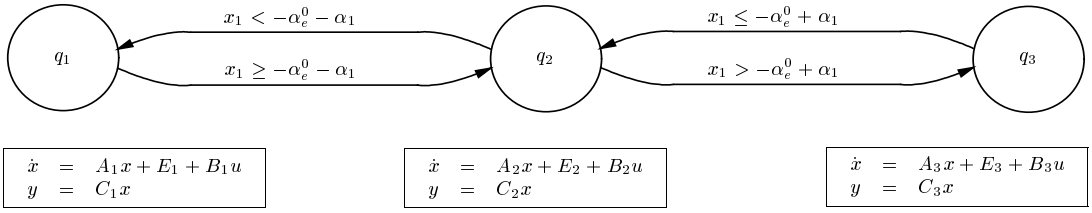


Figure 1: Driveline hybrid model $H_{drvln}$.

accuracy the complex nonlinear effects in the driveline due to the gear backlash, clutch and gear friction and vehicle aerodynamics. After a deep analysis of the model [11], supported by a comprehensive set of simulations and experimental data, we concluded that, for bounded excursions of the vehicle velocity, the most important nonlinearity affecting the behavior of the driveline is that due to the variations of the elasticity of the driveline. Then, for the above mentioned operating conditions, we obtained a reduced–order model whose state variables are: the driveline torsion angle $\alpha_e$, the crankshaft revolution speed $\omega_c$, and the wheel revolution speed $\omega_p$. In this model the driveline nonlinearty is represented by a discontinuity of the elastic coefficient at some value $\alpha_1$ of torsion. See figure 2.

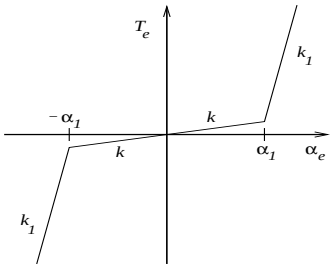


Figure 2: Elastic torque profile.

We consider the equilibrium point $(\alpha_e^0, \omega_c^0, \omega_p^0)^T$ corresponding to 2000 rpm (i.e. $\omega_c^0 = (\pi/30)\,2000$ rad/sec) with second gear engaged. Linearizing aero-dynamics and other remaining nonlinearities around this equilibrium point, the driveline model is expressed as follows

$$\dot{x}(t) = A\,x(t) + E\,T_{sm}(x) + B\,u(t) \quad (1)$$
$$y(t) = C\,x(t) \quad (2)$$

where $x = (\alpha_e - \alpha_e^0, \omega_c - \omega_c^0, \omega_p - \omega_p^0)$, the input $u$ and the feedback $T_{sm}(x)$ stand respectively for the torque generated by the engine and the transmitted torque minus the corresponding equilibrium values. The measurable output $y$ represents the variation of the crankshaft speed with respect to the equilibrium value expressed in rpm. In (1) and (2), we have

$$A = \begin{bmatrix} 0 & \tau & -1 \\ 0 & -\frac{B_e}{J_e} & 0 \\ 0 & 0 & 0 \end{bmatrix}, \quad E = \begin{bmatrix} 0 \\ -\frac{\tau}{J_e} \\ \frac{1}{J_v} \end{bmatrix},$$

$$B = \begin{bmatrix} 0 & \frac{1}{J_e} & 0 \end{bmatrix}^T, \quad C = \begin{bmatrix} 0 & \frac{30}{\pi} & 0 \end{bmatrix},$$

and $T_{sm}(x) = f(x_1) + b_{sm}(\tau x_2 - x_3)$ with, assuming $\alpha_e^0 > \alpha_1$,

$$f(x_1) = \begin{cases} k_1 x_1 + 2(k_1 - k)\alpha_1 & \text{if } x_1 + \alpha_e^0 < -\alpha_1 \\ k x_1 - (k_1 - k)(\alpha_e^0 - \alpha_1) & \text{if } |x_1 + \alpha_e^0| \leq \alpha_1 \\ k_1 x_1 & \text{if } x_1 + \alpha_e^0 > \alpha_1 \end{cases}$$

| | | | |
|---|---|---|---|
| $\tau$ | transmission ratio | $J_v$ | secondary driveline inertia |
| $J_e$ | primary driveline inertia | $B_e$ | primary driveline viscous coef. |
| $b_{sm}$ | driveline viscous coef. | $\alpha_1$ | elasticity discontinuity point |
| $k$ | low driveline elasticity | $k_1$ | high driveline elasticity |

Table 1: Hybrid model parameters.

Model parameters are summarized in Table 1.

The nonlinear driveline dynamics can be represented by a hybrid automaton with 3 locations related to the 3 possible values of the driveline elastic coefficient. The hybrid automaton, referred to as $H_{drvln}$, is depicted in Figure 1. The model parameters are as follows

$$A_1 = A_3 = \begin{bmatrix} 0 & \tau & -1 \\ -\frac{k_1\tau}{J_e} & -\frac{B_e+\tau^2 b_{sm}}{J_e} & \frac{\tau b_{sm}}{J_e} \\ \frac{k_1}{J_v} & \frac{\tau b_{sm}}{J_v} & -\frac{b_{sm}}{J_v} \end{bmatrix},$$

$$A_2 = \begin{bmatrix} 0 & \tau & -1 \\ -\frac{k\tau}{J_e} & -\frac{B_e+\tau^2 b_{sm}}{J_e} & \frac{\tau b_{sm}}{J_e} \\ \frac{k}{J_v} & \frac{\tau b_{sm}}{J_v} & -\frac{b_{sm}}{J_v} \end{bmatrix},$$

$$E_1 = 2(k_1 - k)\alpha_1 E, \quad E_2 = -(k_1 - k)(\alpha_e^0 - \alpha_1)E, \quad E_3 = [0\ 0\ 0],$$
$$B_1 = B_2 = B_3 = B \text{ and } C_1 = C_2 = C_3 = C\,.$$

## 3 Hybrid observer design

In this section, we propose a metodology for the design of a hybrid observer for a generic hybrid plant with no continuous state resets.

Let $H_{plant}$ denote the hybrid automata model of a given hybrid plant (see [5]) with $N$ locations and let $(q, x)$, $(\sigma, u)$ and $(\psi, y)$ stand, respectively, for the hybrid state, inputs and outputs of the plant. We want to design a hybrid observer for the plant $H_{plant}$ that provides an estimate $\tilde{q}$ and an estimate $\tilde{x}$ for the current location $q$ and current continuous state $x$ of $H_{plant}$.

We assume that, in each location $q_i$, the continuous evolution of $x$ is subject to a linear o.d.e.

$$\dot{x} = A_i x + B_i u \quad (3)$$
$$y = C_i x \quad (4)$$

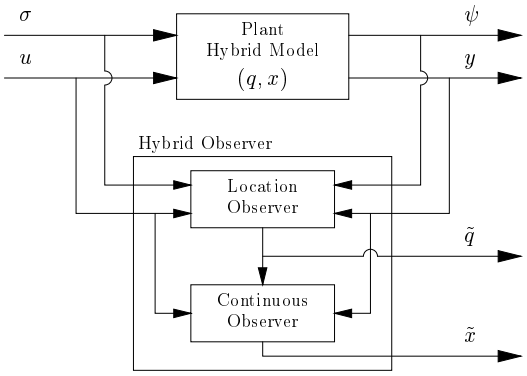


Figure 3: Observer structure: location observer $H_{locobs}$ and continuous observer $H_{cntobs}$ .

with $A_i$, $B_i$ and $C_i$ depending on the location $q_i$. We denote by $N'$ the number of distinct triple $(A_i, B_i, C_i)$.

As design specification for the hybrid observer, we consider the classical exponential convergence in the continuous time domain. Let $\zeta(t)$ be the observation error $\tilde{x}(t) - x(t)$.

**Specification:** Given a neighborhood amplitude $M_0$ and a velocity of convergence $\mu$, the hybrid observer has to produce an evolution of the observation errror $\zeta$ satisfying

$$\|\zeta(t)\| \leq Me^{-\mu t}\|\zeta(0)\| + M_0 \qquad \forall t > 0 \qquad (5)$$

for some $M > 0$.

The structure of the proposed hybrid observer is illustrated in Figure 3. It is composed of two blocks:

1. a *location observer*, and
2. a *continuous observer*.

The *location observer* receives as input the plant inputs $(\sigma, u)$ and outputs $(\psi, y)$. Its task is to provide the estimate $\tilde{q}$ of the discrete location $q$ of the hybrid plant at the current time. This information is used by the *continuous observer* to construct an estimate $\tilde{x}$ of the plant continuous state that exponentially converges to $x$. The continuous plant input $u$ and output $y$ are used by the continuous observer.

In the following sections the location observer and the continuous observer are described in details.

### 3.1 Location observer

Consider first $N'$ locations with distinct dynamics parameters $(A_i, B_i, C_i)$ in (3–4). In this case, the task of the location observer is similar to that of a fault detection and isolation algorithm (see [8] for a tutorial). Indeed, the location observer has to choose which dynamics the continuous system is obeying to in a set of known ones. Assuming that the location observer has properly recognized that the hybrid plant $H_{plant}$ is in location $q_i$, i.e. $\tilde{q} = q_i$, then the location observer should detect a fault from the evolution of $u(t)$ and $y(t)$ when the plant $H_{plant}$ changes the location to some $q_j \neq q_i$ and should identify the new location $q_j$.

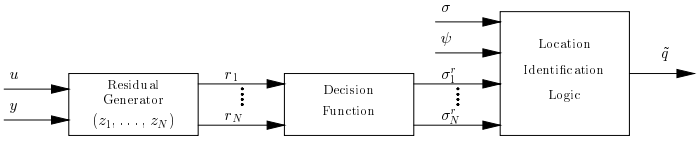


Figure 4: Location observer structure.

The time delay in the location change detection and isolation is critical to the convergence of the overall hybrid observer. We denote by $\Delta$ an upper bound for such delay.

Since when a change of location occurs, the continuous dynamics of the plant suddenly change, then the fault detection algorithms of interest are those designed for abrupt faults [4]. The general scheme is composed of three cascade blocks: the *residual generator*, the *decision function*, and the fault decision logic, renamed here *location identification logic*, see Figure 4.

The simplest and most reliable approach for our application is to use a bank of $N'$ Luenberger observers (see [4]), one for each plant dynamics, as residual generators:

$$\dot{z}_j = H_j z_j + B_j u + L_j y \qquad (6)$$
$$r_j = C_j z_j - y \qquad (7)$$

where $H_j = A_j - L_j C_j$ and $L_j$ are design parameters. The $N'$ residual signals $r_j$ are used as signatures to identify the continuous dynamics the plant is obeying to. Indeed, no–vanishing signatures $r_j(t)$ correspond to $j \neq i$. The decision function outputs $N'$ binary signals as follows:

$$\sigma_j^r = \begin{cases} \textit{true} & \text{if } |r_j| \leq \epsilon \\ \textit{false} & \text{if } |r_j| > \epsilon \end{cases} \qquad \text{for } j = 1, \ldots, N' \quad (8)$$

where the threshold $\epsilon$ is a design parameter.

In the following proposition a sufficient condition for ensuring $\sigma_i^r = \textit{true}$ in a time $\Delta$ after a transition of the hybrid plant $H_{plant}$ to a dynamics $(A_i, B_i, C_i)$ is presented.

**Proposition 3.1.1** *For a given $\Delta > 0, \epsilon > 0$ and a given upper bound $Z_0$ on $\|x - z_i\|$, if the estimator gains $L_i$ in (6) are chosen such that*

$$\alpha(H_i) \leq -\frac{1}{\Delta} \log \frac{n \|C_i\| k(H_i) Z_0}{\epsilon} \qquad (9)$$

*then $\sigma_i^r$ becomes true before a time $\Delta$ elapses after a change in the plant dynamics parameters to the values $(A_i, B_i, C_i)$.*

The following result (see [6]) is instrumental in proving proposition 3.1.1.

**Proposition 3.1.2** *Let $A$ be a matrix in $\mathbb{R}^{n \times n}$ and let $\alpha(A)$ stand for the spectral abscissa (i.e. the maximal real part of the eigenvalues) of matrix $A$. We have*

$$\|e^{A\tau}\| \leq n\, k(A)\, e^{\alpha(A)\tau} \qquad \forall\, \tau \geq 0. \qquad (10)$$

*where $k(A) = \|X\|\,\|X^{-1}\|$ with $X$ such that $X^{-1}AX$ is in the Jordan canonical form.*

**Proof of Proposition 3.1.1.** Assume that the plant hybrid model enters the location $q_i$ at some time $t_0$ and consider the generic $j$–th residual generator (6–7). Introducing $\xi_j = x - z_j$, by (3–4) and (6–7), we have

$$\begin{bmatrix} \dot{x} \\ \dot{\xi}_j \end{bmatrix} = \begin{bmatrix} A_i & 0 \\ M_{ji} & H_j \end{bmatrix} \begin{bmatrix} x \\ \xi_j \end{bmatrix} + \begin{bmatrix} B_i \\ B_{ij} \end{bmatrix} u \quad (11)$$

$$r_j = [C_{ji} \quad C_j] \begin{bmatrix} x \\ \xi_j \end{bmatrix} \quad (12)$$

where $M_{ji} = (A_j - A_i) - L_j(C_j - C_i)$, $B_{ji} = B_j - B_i$, $C_{ji} = C_j - C_i$. Since, $M_{ii}$, $B_{ii}$ and $C_{ii}$ are null matrices, by (12–11) we have

$$r_i(t) = C_i e^{H_i(t-t_0)}\xi_i(t_0) \quad (13)$$

Hence, to achieve an estimation of the new plant location within a time smaller than a given $\Delta$, the transient evolution in (13) should be smaller than $\epsilon$ when $t - t_0 > \Delta$, so to have $\sigma_i^r = \textit{true}$ according to (8). This can be always obtained by selecting the estimation dynamics (6) fast enough. In fact, by (10) the residuals (13) can be bounded as follows

$$\begin{aligned} |r_i(t)| &\leq \|C_i\|\|e^{H_i(t-t_0)}\|\,\|\xi_i(0)\| \\ &\leq \|C_i\| n\, k(H_i)\, e^{\alpha(H_i)(t-t_0)}\|\xi_i(0)\| \\ &\leq \|C_i\| n\, k(H_i)\, e^{\alpha(H_i)\Delta} Z_0 \qquad \forall\, t \geq t_0 + \Delta, \end{aligned}$$

which gives $|r_i(t)| < \epsilon$ for $t \geq t_0 + \Delta$, provided that $L_i$ is chosen according to (9). **Q.E.D.**

Let us now consider the $j$–th residual generator and let us assume that the continuous state $x$ of $H_{\textit{plant}}$ is obeying the dynamics defined by parameters $(A_i, B_i, C_i)$ with $i \neq j$. Unfortunately, as shown by the following proposition, there are cases where we cannot prevent the signal $\sigma_j^r$ from being *true* for an unbounded time:

**Proposition 3.1.3** *If the matrix $C_{ji}B_i + C_jB_{ij}$ is invertible, with $i \neq j$, then for any hybrid plant initial condition, the class of plant inputs $u$ that achieves $\sigma_j^r = \textit{true}$ after a time $\Delta$ after a change in the plant dynamics parameters to $(A_i, B_i, C_i)$ is not empty.*

**Proof of Proposition 3.1.3.** Introduce the region

$$R_{x\xi_j} = \left\{(x, \xi_j) \in \mathbb{R}^{2n} | -\epsilon \leq [C_{ji} \quad C_j](x, \xi_j) \leq \epsilon\right\}. \quad (14)$$

By (12) we have have that if $(x(t), \xi_j(t))$ belongs to $R_{x\xi_j}$, then the decision generator (8) outputs a true value both for $\sigma_i^r$ and $\sigma_j^r$. If $C_{ji}B_i + C_jB_{ij}$ is invertible, then the necessary and sufficient condition for establishing a slinding motion on the surface $[C_{ji} \quad C_j](x, \xi_j) = 0$ for the plant dynamics (11) is satisfied. Then, by (12), there exists a particular control that can steer the system to the subspace where $r_j = 0$ in time less than $\Delta$, and maintain its motion on it, with the result of having $\sigma_j^r = \textit{true}$ for all $t > t_0 + \Delta$.

**Q.E.D.**

In the general case, the set of configurations and the class of plant inputs for which the signatures (12) fail to properly identify the continuous dynamics when a time $\Delta$ is elapsed after a plant discrete transition can be obtained by computing the maximal safe set and the maximal controller for dynamics (11) with respect to a safety specification defined in an extended state space that contains an extra variable $\tau$ representing the elapsed time. More precisely, the set of configurations for which a wrong signature is produced up to a time $t' > \Delta$ after a change of location of the plant, is given by those configurations $(\tau^0, x^0, \xi_j^0)$ from which there exists a plant continuous input $u$ able to keep the trajectory inside the set $\mathbb{R}^{2n+1} \setminus [\Delta, t') \times R_{x\xi_j}$.

The location identification logic receives the $N'$ signals $\sigma_j^r$ and the discrete plant inputs $\sigma$ and outputs $\psi$, if available. Based on this information it has to return the value $\tilde{q}$ of the estimated plant location. The critical cases the identification algorithm should solve are the following ones

- more than one signal $\sigma_j^r$ is true at a same time;
- only one signal $\sigma_j^r$ is true but the dynamic parameters $(A_j, B_j, C_j)$ are associtated to more than one plant location.

Such problems can be addressed exploiting the structure of the plant automaton and using FSM identification algorithms, which take advantage of the informations coming from the continuous evolutions of the hybrid plant, provided by signals $\sigma_j^r$, as well as from the discrete plant inputs $\sigma$ and outputs $\psi$.

### 3.2 Continuous observer

The continuous observer is a hybrid system, referred to as $H_{\textit{cntobs}}$, whose dynamicss depend on the current estimate $\tilde{q}$ of the hybrid plant location $q$ provided by the location observer. The scheme of the continuous observer is readily obtain using the classical Luenberger's approach [7]:

$$\dot{\tilde{x}}(t) = F_i\tilde{x}(t) + B_iu(t) + G_iy(t) \quad \text{if } \tilde{q} = Q_i. \quad (15)$$

where $F_i = (A_i - G_iC_i)$. If $q = Q_i$, the corresponding dynamics of the observation error $\zeta = \tilde{x} - x$ is $\dot{\zeta}(t) = F_i\zeta(t)$. The gain matrix $G_i$ is the design parameter used to set the velocity of convergence in each location.

It is worth noting that the Luenberger observers (6) contained in the residual generators, which are designed to convergence to the same state variable $x$, do not provide a satisfactory estimate of the evolution of $x$ since they are tunning according to (9) in order to meet the specification of producing a residual with a transient time less than $\Delta$. Hence, they exhit a high overshoot which is undesiderable for feedback purpose. This is the reason why we have to add a further observer, (15), for constructing a reliable estimate $\tilde{x}$ of the continuous state $x$.

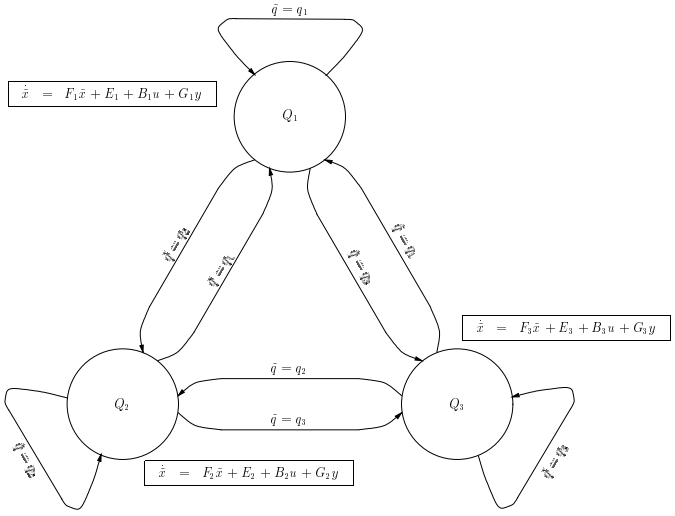


Figure 5: Continuous hybrid observer scheme $H_{cntobs}$.

The hybrid model of the continuous observer $H_{cntobs}$ for the driveline model $H_{plant}$, described in section 2, is reported[1] in Figure 5.

### 3.3 Exponentially convergent hybrid observer

The properties of convergence of the hybrid observer are studied considering the complete hybrid system, denoted $H_{plantobs}$, obtained by composing the hybrid model $H_{plant}$ and the observer hybrid model $H_{locobs}$ and $H_{cntobs}$. The hybrid system $H_{plantobs}$ has $N' \times N'$ locations (9 for the driveline case). The locations are labeled $(q_i, Q_j)$, the former corresponding to plant locations and the latter corresponding to observer locations. To each location $(q_i, Q_j)$, the continuous dynamics

$$\begin{aligned} \dot{x}(t) &= A_i x(t) + B_i u(t) && (16)\\ \dot{\zeta}(t) &= F_j\zeta(t) + [(A_i - A_j) - G_j(C_i - C_j)]\, x(t) \\ &\quad +(B_i - B_j)u(t) && (17)\end{aligned}$$

is associated. By integrating (17) we have

$$\zeta(t) = e^{F_j t}\zeta(0) + e^{F_j t} \star v(t) \qquad (18)$$

where $\star$ denotes the convolution operator and

$$v(t) = [(A_i - A_j) - K(C_i - CJ)]\, x(t) + (B_i - B_j)u(t)$$

The following notation will be used in the sequel (see e.g. [12])

- $\|m(t)\|_\infty = \max_{k=1,q}\ \sup_{t\geq 0} |m_k(t)|$, $L^\infty$–norm of $q$–dimensional signals $m : \mathbb{R} \to \mathbb{R}^q$;
- $\|M\|_\infty, \|M\|_1$ $L^\infty$ and the $L^1$–norm of a matrix $M$.

**Proposition 3.3.1** *Assume that the hybrid system $H_{plant}$ exhibits transitions with time separation greater than or equal to some $D > 0$. Assume also that all the couples $(A_i, C_i)$ are observable, $\|x(t)\|_\infty \leq X$, for some $X > 0$ and $\|u(t)\|_\infty \leq X$, for some $U > 0$ so that*

$$\begin{aligned} \|v(t)\|_\infty \leq V &= \| [(A_i - A_j) - G_j(C_i - C_j)] \|_1 X \\ &\quad +\|B_i - B_j\|_1 U \qquad (19)\end{aligned}$$

*Given a value $\mu > 0$, if the location observer $H_{locobs}$ identifies a change in the hybrid system location within time $\Delta < D$, there exist gains $G_i$ such that the state $\tilde{x}$ of the continuous observer $H_{cntobs}$ converges to the set*

$$\|x - \tilde{x}\| \leq M_0 = \frac{nk(F_j)V\Delta}{1 - e^{\alpha(F_j)D}} \qquad (20)$$

*with velocity of convergence greater than $\mu$.*

Consider the first two subsequent transitions of the hybrid plant $H_{plant}$, occurring at times $t_1$ and $t_2$ respectively. By hypothesis

$$t_2 - t_1 \geq D. \qquad (21)$$

Since $\Delta < D$, the location observer $H_{locobs}$ identifies the state transitions at some time $t_1'$ and $t_2'$ with $t_1' - t_1 \leq \Delta$ and $t_2' - t_2 \leq \Delta$. Hence, by (21), $t_2 - t_1' \geq D - \Delta > 0$. Since $Q = q$ in the time interval $[t_1', t_2]$, then, by properly choosing $G_i$, convergence to zero of $\zeta(t)$ at any desired velocity can obtained. However, since $Q \neq q$ when $t \in [t_2, t_2']$, $\zeta(t)$ may fail to converge later. Hence, the convergent behavior for $t \in [t_1', t_2]$ has to compensate the divergent behavior for $t \in [t_2, t_2']$.

By (18), we have

$$\zeta(t) = e^{F_j(t-t_1')}\zeta(t_1') \qquad \forall t \in [t_1', t_2] \qquad (22)$$

$$\zeta(t) = e^{F_j(t-t_1')}\zeta(t_1') + \int_0^{t-t_2} e^{F_j(t-t_2-\tau)} v(\tau + t_2)\, d\tau \qquad \forall t \in (t_2, t_2'] \qquad (23)$$

Since, by (10), $\|e^{F_j\tau}\| \leq nk(F_j)e^{\alpha(F_j)\tau}$, then for all $t \in [t_1', t_2]$ the evolution of $\zeta(t)$ for can be bounded as follows

$$\|\zeta(t)\| \leq nk(F_j)e^{\alpha(F_j)(t-t_1')}\|\zeta(t_1')\| \qquad (24)$$

Inequality (24) provides also an upper bound for the first term in (23). For the second term, we have

$$\begin{aligned} &\left\| \int_0^{t-t_2} e^{F_j(t-t_2-\tau)} v(\tau + t_2)\, d\tau \right\| \\ &\leq nk(F_j) \int_0^{t-t_2} e^{\alpha(F_j)(t-t_2-\tau)} \|v(\tau + t_2)\|\, d\tau \\ &\leq nk(F_j)\|v(t)\|_\infty \int_0^{t-t_2} e^{\alpha(F_j)\tau}\, d\tau \\ &= nk(F_j)V\, \frac{e^{\alpha(F_j)(t-t_2)} - 1}{\alpha(F_j)} \leq [nk(F_j)V](t - t_2) \qquad (25)\end{aligned}$$

Then, using (23),(24) and (25), we have that, $\forall t \in (t_2, t_2']$,

$$\|\zeta(t)\| \leq e^{\alpha(F_j)(t-t_1')}\|\zeta(t_1')\| + [nk(F_j)V](t - t_2) \qquad (26)$$

[1] Note that in this model the constant terms $E_i$ have been added.

Consider the worst case in which the location observer takes exactly time $\Delta$ to identify a change in the hybrid system location and the hybrid plant exhibits transitions with time separation equal to $D$. Then, by (26) with $t = t'_2$ and (20) we have

$$\|\zeta(t'_2)\| \leq e^{\alpha(F_j)D}\|\zeta(t'_1)\| + nk(F_j)V\Delta \qquad (27)$$

Hence, assuming $\|\zeta(t'_1)\| = M_0$, from (27) we obtain

$$\|\zeta(t'_2)\| \leq e^{\alpha(F_j)D}M_0 + nk(F_j)V\Delta = M_0$$

This shows that the hybrid observer keeps $\|x - \tilde{x}\|$ below the bound $M_0$ given by (20) when convergence is achieved.

To prove that the observation error $\zeta(t)$ converges to this set with velocity greater than $\mu$, we have to show that

$$\|\zeta(t'_2)\| \leq e^{-\mu(t'_2 - t'_1)}\|\zeta(t'_1)\| \qquad (28)$$

when $\|\zeta(t'_1)\| > M_0$. The worst case for the above inequality is given by $t'_2 - t'_1 = D$. Hence, by (27), we have that velocity of convergence $\mu$ is achieved if $G_i$ are chosen such that

$$e^{\alpha(F_j)D}\|\zeta(t'_1)\| + nk(F_j)V\Delta \leq e^{-\mu D}\|\zeta(t'_1)\|$$

is satisfied. **Q.E.D.**

Figure 6 shows some simulation results for a hybrid observer of the driveline model presented in Section 2. The figure shows the dynamics of $\alpha_e(t) - \alpha_e^0$, with $\alpha_e^0 = 0.025$ rad, when at time $t = 2$ a negative step of 10 Nm is applied with respect to the equilibrium torque generated by the engine. Since $\alpha_1 = 0.015$ rad, then a change of location occurs when $\alpha_e(t) - \alpha_e^0$ reaches one of the thresholds $-\alpha_e^0 + \alpha_1 = -0.01$ rad, $-\alpha_e^0 - \alpha_1 = -0.04$ rad. Signals $\sigma_2^r$ and $\sigma_3^r$ are also depicted in Figure 6. Note that the raising edges of the signals $\sigma_2^r$ and $\sigma_3^r$ detect, with a negligible delay $\Delta$, the driveline location changes so that the Location Identification Logic is able to recognize, with the same delay, the true location of the system.

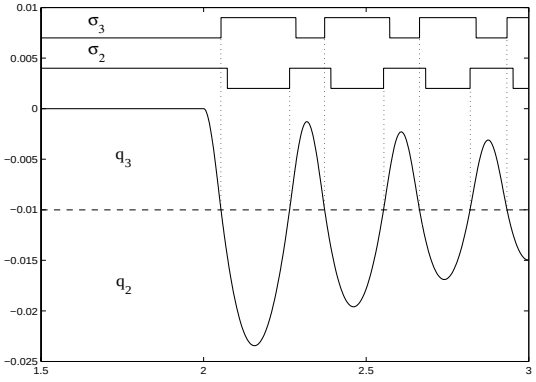


Figure 6: Driveline torsion angle variation w.r.t. the equilibrium value and signals $\sigma_2^r$, $\sigma_3^r$.

## Acknowledgements

This research has been partially sponsored by PARADES, a Cadence, Magneti-Marelli and SGS-Thomson E.E.I.G, and by CNR PF–MADESSII SP3.1.2 .

## References

[1] A. Balluchi, L. Benvenuti, M. D. Di Benedetto, C. Pinello, and A. L. Sangiovanni-Vincentelli. Automotive engine control and hybrid systems: Challenges and opportunities. *Proceedings of the IEEE*, 88, "Special Issue on Hybrid Systems" (invited paper)(7):888–912, July 2000.

[2] A. Balluchi, M. D. Di Benedetto, C. Pinello, C. Rossi, and A. L. Sangiovanni-Vincentelli. Hybrid control in automotive applications: the cut-off control. *Automatica*, 35, Special Issue on Hybrid Systems:519–535, March 1999.

[3] A. Balluchi, M. D. Di Benedetto, C. Pinello, and A. L. Sangiovanni-Vincentelli. A hybrid approach to the fast positive force transient tracking problem in automotive engine control. In *Proc. 37th IEEE Conference on Decision and Control*, pages 3226–3231, Tampa, Florida, USA, December 1998.

[4] P. M. Frank. Fault diagnosis in dynamic systems using analytical and knowledge–based redundancy — a survey and some new results. *Automatica*, 26(3):459–474, 1990.

[5] Thomas A. Henzinger. The theory of hybrid automata. Technical Report UCB/ERL M96/28, Electronics Research Laboratory, University of California, Berkeley, May 1996.

[6] C. Van Loan. The sensitivity of the matrix exponential. *SIAM Journal of Number Analysis*, 14(6):971–981, December 1977.

[7] D.G. Luenberger. An introduction to observers. *IEEE Transactions on Automatic Control*, 16(6):596–602, Dec 1971.

[8] M.-A. Massoumnia, G.C., Verghese, and A.S. Willsky. Failure detection and identification. *IEEE Transactions on Automatic Control*, 34(3):316–21, March 1989.

[9] C. Y. Mo, A. J. Beaumont, and N. N. Powell. Active control of driveability. Technical Report 960046, SAE, 1996.

[10] M. Pettersson, L. Nielsen, and L. G. Hedström. Transmission-torque control for gear shifting with engine control. Technical Report 970864, SAE, 1997.

[11] Annalisa Scacchioli. Sintesi di un osservatore per una catena di trasmissione meccanica. "laurea" thesis, Università degli Studi di L'Aquila, Poggio di Roio, 67040 L'Aquila, Italy, 2000.

[12] M. Vidyasagar. *Nonlinear Systems Analysis*. Prentice–Hall, Inc, Englewood Cliffs, N.J., 1978.